Enhancement of the modulus of compression of calcium silicate hydrates via covalent synthesis of CNT and silica fume

G.M. Kim [a,1], Y.K. Kim [b,1], Y.J. Kim [b], J.H. Seo [c], B.J. Yang [b], H.K. Lee [c,*]

[a] Korea Institute of Geoscience and Mineral Resources, 124 Gwahak-ro, Yuseong-gu, Daejeon 34132, Republic of Korea
[b] Institute of Advanced Composite Materials, Korea Institute of Science and Technology, 92 Chundong-ro, Bongdong-eup, Wanju-gun, Jeollabuk-do 55324, Republic of Korea
[c] Department of Civil and Environmental Engineering, Korea Advanced Institute of Science and Technology, 291 Daehak-ro, Yuseong-gu, Daejeon 34141, Republic of Korea

HIGHLIGHTS

- CNT and silica fume were covalently synthesized.
- Synthesized CNT and silica fume incorporated cement composites were fabricated.
- Covalently synthesized CNT and silica fume improved the stiffness of C-S-H.
- Covalently synthesized CNT and silica fume significantly enhanced mechanical strength.

ARTICLE INFO

ABSTRACT

The effects of covalently synthesized CNT and silica fume on the modulus of compression of calcium silicate hydrates were investigated in the present study. For the conjugation of CNT and silica fume, the surfaces of silica fume and CNT were functionalized with a primary amine group and a carbonyl chloride group, respectively. The aminated silica fume and carbonyl chloride functionalized CNT were covalently bonded by the formation of amide bridges. The characteristics of the covalently synthesized CNT and silica fume were investigated via zeta potential, Fourier-transform infrared spectroscopy, scanning electron microscopy, Raman spectroscopy and sedimentation tests. The compressive strength and modulus of compression of calcium silicate hydrates of cementitious composites incorporating the synthesized CNT and silica fume were then investigated. The test results showed that the addition of the synthesized CNT and silica fume improved the stiffness of calcium silicate hydrates, thereby significantly increasing the compressive strength of the composites.

© 2018 Published by Elsevier Ltd.

1. Introduction

Various supplementary cementitious materials including silica fume, blast furnace slag, fly ash and metakaolin have been widely adopted to improve the mechanical properties of cementitious composites [33,36]. Silica fume is one of the most representative additives and has been utilized as a supplementary cementitious material since the 1970s. Its specific gravity and bulk density are approximately 2.20 and in the range of 200–300 kg/m³, respectively [36]. Previous studies reported that the content of silica fume that is able to improve the mechanical properties of cementitious materials is 5.0–10.0% by the weight of cement and that the compressive strength of cementitious materials increased by 10–50%, relative to that of specimens without silica fume [30,32,36].

The addition of silica fume induces particle packing, which thus densifies the matrix of cementitious materials [3]. Dual et al. reported that the silica fume reduces the total porosity of cementitious materials by approximately 4.0% [7]. Furthermore, it has been demonstrated that silica hydrate conversion facilitates porosity reduction [36] and that the silica fume added in cementitious materials reacts with $Ca(OH)_2$ and forms a calcium silicate hydrate (C-S-H) phase which is a major hydration product responsible for the mechanical properties of cementitious materials [3,7,36]. Thus, the mechanical properties of cementitious materials can be vastly improved by the incorporation of silica fume [3,7,36].

As nanotechnology has been an issue, studies on the enhancement of the mechanical properties of cementitious materials that utilize nanomaterials have been actively attempted. Carbon

---

nanotube (CNT) is one of the most promising nanomaterials that has been applied to improve the mechanical properties of cementitious materials. This material has remarkable mechanical, electrical and thermal properties [34,2,41]. In particular, the Young's modulus of this material is approximately 1.0–1.8 TPa [38], as each C atom in the structure of CNT is composed of C—C bonds, among the strongest bonds in nature [10]. The major issues related to improvement of the mechanical properties of CNT-reinforced cementitious composites are the dispersion of the CNT and the bond strength between the CNT particles and the hydrates [11,12]. Various methods including ultrasonication, the use of surfactants and siliceous materials, and surface modifications of CNT have been proposed to disperse CNT effectively in cementitious composites [17,16,4,14,24,12].

In previous studies, the increase in the compressive strength of cementitious materials with CNT was reported to be in the range of 10–20% and a suitable range of content that can be added to cementitious materials to improve the compressive strength was given as 0.01–0.15% by the weight of cement [9,18,23,28]. The addition of CNT can affect the microstructural properties and the characteristics of C-S-H phase. Nochaiya and Chaipanich reported that the addition of CNT to cementitious materials reduced the porosity by more than 4.0%, mainly decreasing mesopores in the matrix [27]. Meanwhile, Konsta-Gdoutos et al. reported that CNT added to cementitious materials contributed to the improved stiffness of the C-S-H phase [17,16]. However, a large amount of CNT may inhibit the hydration reaction and reduce the mechanical properties [23]. Morsy et al. reported that CNT particles led to the separation of cement grains as the particles wrapped around grains [23]. Consequently, the bond strength among hydrates was reduced [23].

Several researchers have attempted to devise synthesis methods for CNT and pozzolanic materials to improve the dispersion of CNT in cementitious composites and to enhance the mechanical properties of the composites [25,26]. Nasibulin et al. synthesized CNT and cement particles and reported that the addition of the synthesized material improved the mechanical properties of cementitious composites nearly twofold when the content of the material added to the composites equaled 100% by the weight of cement [26]. Mudimela et al. introduced a simple chemical vapor deposition method to resolve the significantly poor bonding between CNT and cement or silica materials by growing carbon nanomaterials on the surface of target matrix [25]. It should however be noted that synthesized CNT and cement particles reported in the previous studies exhibited a decrease in the mechanical strength at an early age as their dosage increased due to the low degree of hydration of modified cementitious composites [25,26]. Furthermore, a slight enhancement in the mechanical strength was observed only for the samples with a very high fraction of synthesized composites wherein the efficiency of the fabrication may have vulnerability.

The effects of covalently synthesized CNT and silica fume (SF) (hereafter, covalently synthesized CNT and SF is referred to as C-SF) on the mechanical properties of cementitious composites were investigated in the present study. For the conjugation of CNT and SF, the surfaces of the SF and CNT were functionalized with a primary amine group and a carbonyl chloride group, respectively, and the aminated SF and carbonyl chloride functionalized CNT were covalently bonded by the formation of amide bridges. The physicochemical characteristics of the C-SF were investigated via the zeta potential, Fourier-transform infrared spectroscopy, scanning electron microscopy, Raman spectroscopy, and sedimentation tests. The mechanical properties of the composites incorporating the C-SF were investigated.

2. Experimental procedure

2.1. Sample preparation

The mix proportion of cementitious composites incorporating C-SF is provided in Table 1. Type I Portland cement was used as a binder material. A polycarboxylate-type superplasticizer was used to improve the workability and the dispersion of the C-SF in the cementitious composites. The C-SF was manually ground via mortar and pestle and formulated into a solution of C-SF (designated amount) and water (250 g). The solution was then sonicated by means of a bath-type ultrasonicator (200 W, 40 kHz) for 1.5 h to improve the dispersion of the C-SF. The added content of C-SF was varied from 0.15 to 0.5% by the weight of cement and the water to cement (w/c) ratio was fixed at 0.25, since minimization of the w/c ratio can improve the bond strength between hydrates and C-SF, and inhibit re-agglomeration of C-SF [13]. The mixing procedure of the cementitious composites incorporating C-SF was as follows: the cement and water (500 g) were mixed in a Hobart mixer for 1 min and the sonicated solution including C-SF was added. The mixture was further mixed for 5 mins and poured into a prismatic mold 40 × 40 × 160 mm in size, as described in ASTM C348. The specimens were demolded after 24 h and cured at 25 ± 3 °C for 28 days.

2.2. Test methods

The characterization of the C-SF was conducted via zeta potential analyzer (Malvern, Nano ZS), Fourier-transform infrared (FT-IR) spectroscopy (Thermo Scientific, Nicolet iN10 microscopy), field emission-scanning electron microscopy (FE-SEM, HITACHI SU5000) images, Raman spectroscopy (NTEGRA, NT-MDT), and sedimentation tests. The sedimentation test was conducted with solutions denoted as C-SF and pristine CNT to evaluate the dispersion characteristics of C-SF. Each solution was formulated with 8 mL of water and 0.2 g of the selected particles (C-SF or pristine CNT) and sonicated by means of a bath-type ultrasonicator (200 W, 40 kHz) for 1.5 h and observed the sedimentation state of the particles at designated periods.

Cementitious composites having dimensions of 40 mm × 40 mm × 40 mm were used to assess compressive strength. The effects of the C-SF on the nanomechanical characteristics of cementitious composites were investigated by nanoindentation and SEM tests. For the nanoindentation tests, a berkovich tip with an angle of 65° was used and the samples of the cementitious composites with C-SF were prepared in a mold of 5 mm × 5 mm × 2 mm. The samples used in the nanoindentation test were immersed in acetone and were then put into a vacuum desiccator for 48 h to arrest any additional hydration. The samples were carefully polished with silicon carbide paper (#4000) for more than 30 min, and an air compressor was used to remove the polishing debris from the surfaces of the samples, since the surface condition of the samples can significantly affect the results of nanoindentation tests. The test of each sample consisted of 25 indents performed on a 5 × 5 grid (10 μm between each grid point) with a target depth of 5000 nm. Five different areas were arbitrarily selected and the procedure was repeatedly conducted for each sample. That is, the results of 125 indentation tests for each sample were obtained.

3. Covalent synthesis of CNT and SF

Multi-walled CNT (produced by Hyosung Inc. Korea) and SF (EMS-970, manufactured by Elkem Inc.) were used to covalently synthesize CNT and SF. The purity of the CNT exceeded 95%, and the specific gravity, length, and diameter were 1.32, 10 μm, and from 12 to 40 nm, respectively. The corresponding specific gravity, specific surface area, and diameters of the SF were 2.1, 15.0 m^2/g and from 50 to 250 nm. It should be noted that the covalent synthesis of CNT and SF was mainly carried out via one of the following two methods: (1) the synthesis of aminated SF and (2) the synthesis of functionalized CNTs and their covalent coupling in which these methods were referenced from Phonthammachai et al. and Kim and Min, respectively [29,15]. To synthesize the aminated SF, 5 g of SF was dispersed in a 5 L mixture of ethanol to water (at a volume ratio of 3:1) under sonication for 15 mins. Subsequently, 35 mL of 3-aminopropyltriehoxysilane (APTES) was added to the mixture, and it was then stirred at 95 °C for 1 h. After cooling to room temperature, the mixture was centrifuged at 8000 rpm, washed three times with ethanol and water, after which it was dried at 100 °C under a vacuum overnight for future use.

To synthesize CNT functionalized with carbonyl chloride groups, 1 g of CNT was dispersed in 400 mL at a 1:3 ratio of concentrated nitric acid and sulfuric acid, and the mixture underwent

Table 1

Mix proportion of cementitious composites incorporating covalently synthesized CNT and silica fume (g).

Specimen[a]	Cement	C-SF	Silica fume	Water
OPC	2000	–	–	500
SF	2000	–	10	500
C-SF0.15	2000	3	–	500
C-SF0.25	2000	5	–	500
C-SF0.5	2000	10	–	500

[a] The following denotations were used to identify samples: 'OPC', 'SF' and 'C-SF' denote the sole use of ordinary Portland cement, incorporation of silica fume, and incorporation of covalently synthesized CNT and silica fume, respectively, while the numbers following C-SF denote their mass ratio (%) by the weight of cement.
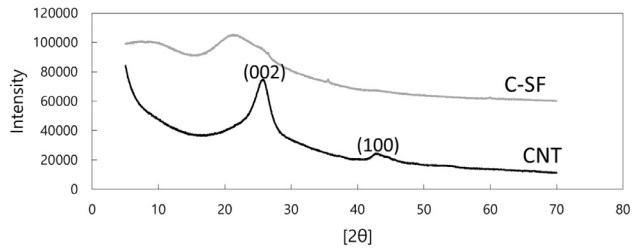

Fig. 1. XRD patterns of pristine CNT and covalently synthesized CNT and silica fume.

sonication for 6 h by using bath-sonicator (200 W, 40 kHz). After sonication, the acidic mixture containing the CNT was centrifuged at 12,000 RPM for 10 min and washed with water. This step was repeated until the supernatant of the centrifuged mixture was neutralized. The obtained CNT was dried at 75 °C under a vacuum overnight. Then, the CNT was dispersed in 50 mL of anhydrous N, N-dimethylformamide (DMF) by sonication for 15 min with continuous nitrogen purging. Then, 450 mL of thionylchloride was quickly added to the DMF mixture including CNT. The temperature of the mixture 95 °C for 24 h while being stirred with continuous nitrogen purging. After the reaction, the excess thionylchloride was removed by rotary evaporation.

To covalently synthesize CNT and SF, 1 g of carbonyl chloride activated CNT was dispersed in 1 L of DMF by bath-sonication for 30 min and 3 g of aminated SF was added to the mixture. The mixture was further sonicated for 1.5 h and stirred for 24 h at 95 °C with continuous nitrogen purging. After the reaction, the mixture was centrifuged at 8000 rpm and washed three times with DMF and ethanol. The obtained C-SF was dried at 75 °C under a vacuum overnight.
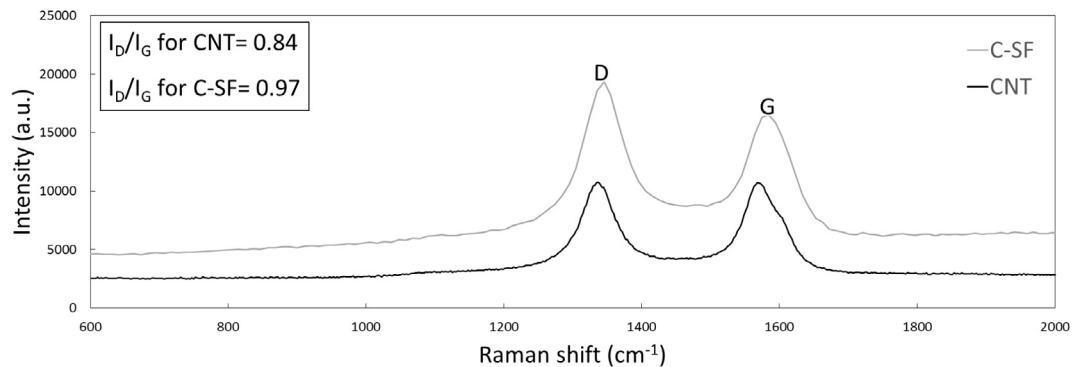
Fig. 2. Raman spectrum results of CNT and covalently synthesized CNT and silica fume.
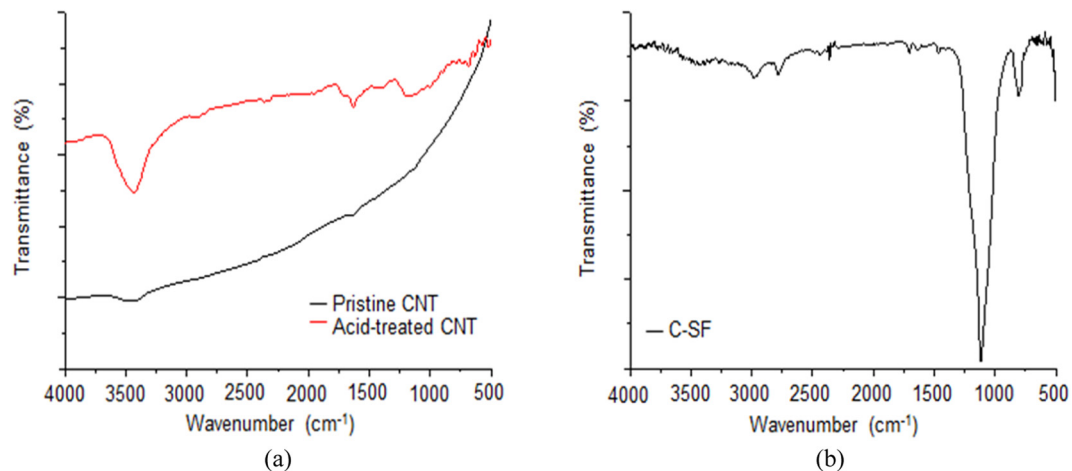
Fig. 3. FT-IR spectra of (a) pristine and acid-treated CNT and (b) covalently synthesized CNT and silica fume.
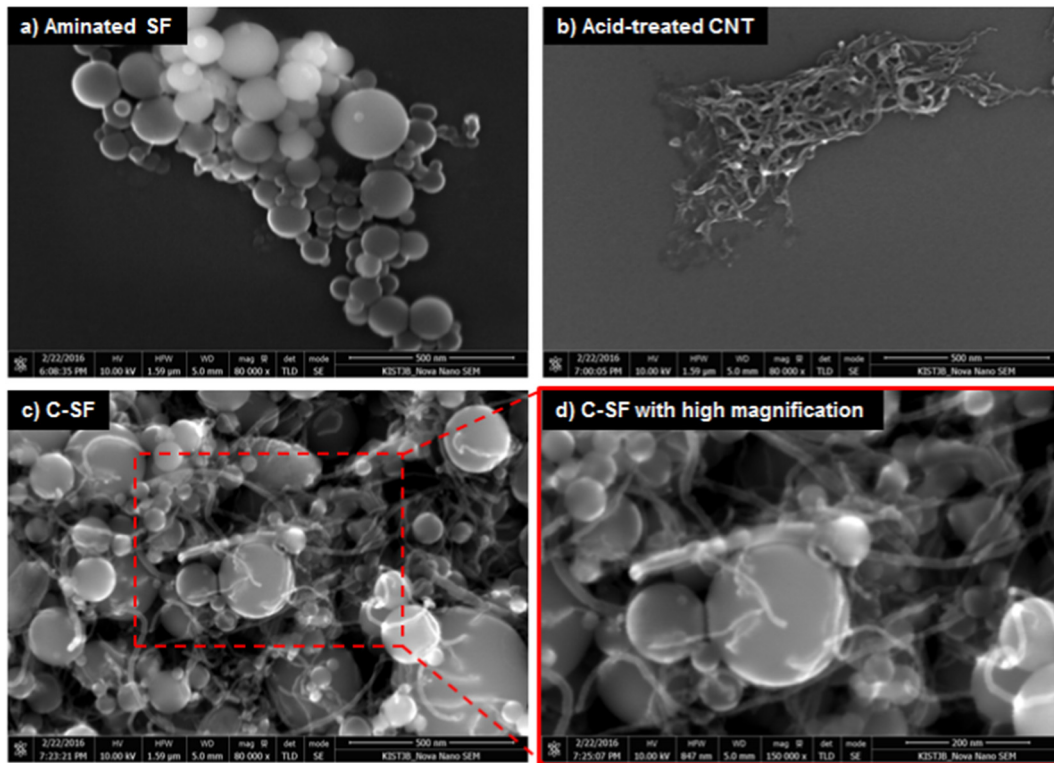
Fig. 4. SEM images of aminated SF (a), acid-treated CNT (b) and covalently synthesized CNT and silica fume (c, d) under different magnification levels.
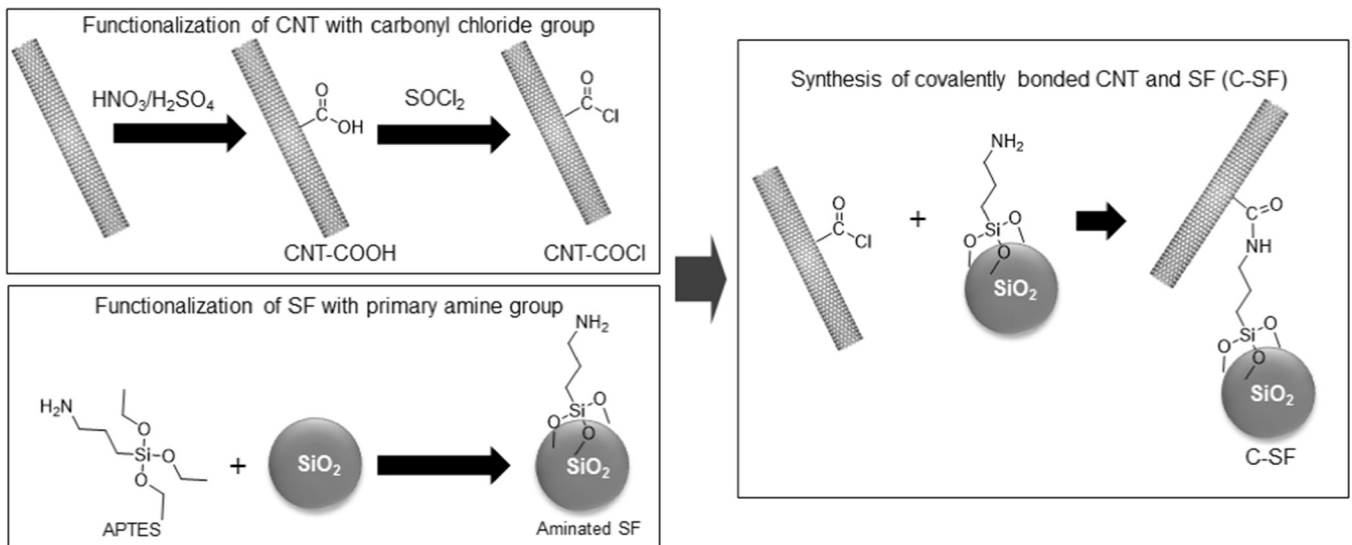

Fig. 5. Synthetic schemes of carbonyl chloride-functionalized CNT, aminated SF and their hybrid structures (covalently synthesized CNT and silica fume).

4. Characterization of C-SF

The measured zeta potential value of SF was -26.7 ± 0.4 eV, and this value increased to 19.5 ± 0.3 eV by APTES treatment. The positive charge of SF suggested that primary amine groups were successfully introduced onto the surface of the SF. For the CNT, the pristine CNT was not dispersible in water; thus its zeta potential could not be measured. In contrast, the acid-treated CNT was dispersed in water and its zeta potential was -30.4 ± 0.4 eV. This negative charge implied that the surface of the CNT was oxidized by the bath-sonication process in the acid mixture. As expected, the zeta potential of C-SF was measured to be -10.8 ± 1.5 eV; this value was close to the sum of the surface charges of the aminated-SF and acid-treated CNT and suggested that they formed a complexed structure.

XRD patterns of the pristine CNT and C-SF samples are shown in Fig. 1. The $(0\,0\,2)$ peak at $25.4°$ in the pattern of the pristine CNT sample corresponds to the space between the graphitic layers in the carbonaceous materials. In the previous study, the 2θ peak involved in the hexagonal carbon nanotube was $26.3°$; this implies that the CNT used in the present study contained impurities [19]. The $(0\,0\,2)$ peak in the pattern of the C-SF sample was broadened
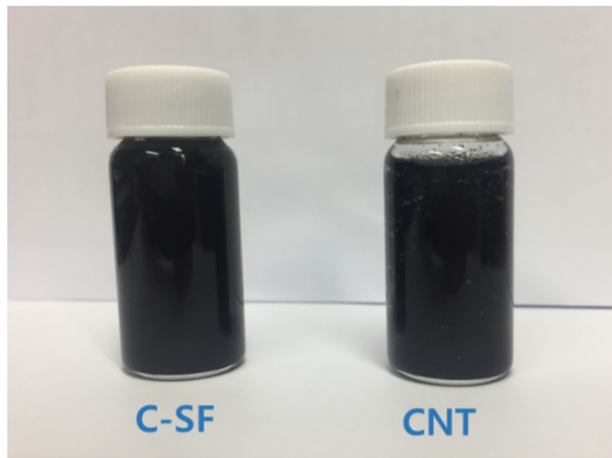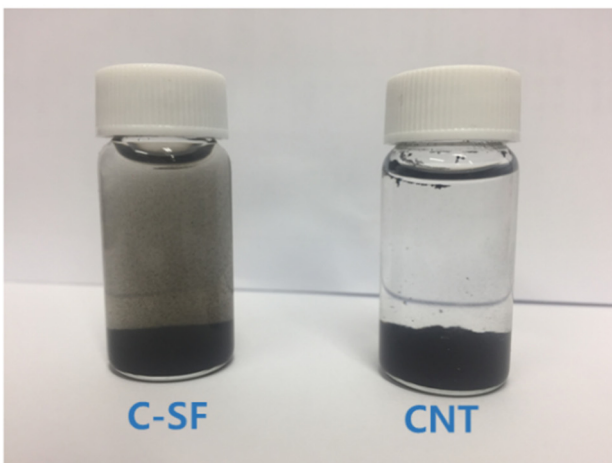
(a)
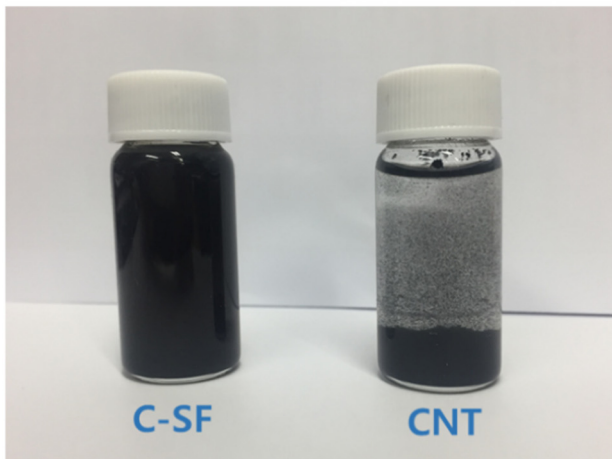
(b)

(c)

Fig. 6. Sedimentation test results of aqueous solutions with covalently synthesized CNT and silica fume and pristine CNT: (a) 0 min, (b) 3 min and (c) 2 h.

compared to that in the pattern of the pristine CNT. This type of broadening is commonly caused by the functionalization process, during which the strain between the graphitic layers increased and the number of the layers is reduced [21]. The (1 0 0) peak at
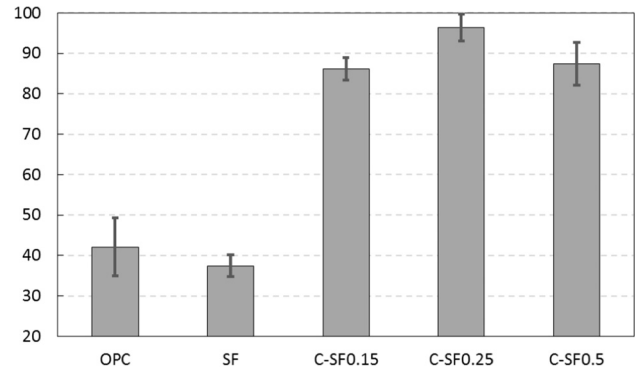
Fig. 7. Compressive strength test results of cementitious composites incorporating covalently synthesized CNT and silica fume at 28 days.

43.6° represents the presence of curved graphene sheets consisting of CNT structures, and the peak intensity is determined by diffraction from the in-plane regularity [21]. The (1 0 0) peak was clearly observed in the pattern of the pristine CNT sample, while the peak was not observed in the pattern of the C-SF sample. The disappearance of the (1 0 0) peak in the C-SF sample is caused by the functionalization process used in the present study. Meanwhile, it is well known that the amorphous hump at 15–30° in the 2θ direction represents SF [1].

Fig. 2 shows the Raman spectra of pristine CNT and the C-SF samples. The spectrum of CNT contained two characteristic peaks (the D and G bands). The D band ($\approx$1,342 cm^{-1}) is generated by the presence of disorder in sp2 hybridized carbon systems, while the G band ($\approx$1,575 cm^{-1}) is caused by the stretching of the C—C bonds [24]. That is, the intensity of the D (I_D) band increases as the defect density increases. Thus, the crystalline quality of CNT can be evaluated with the I_D/I_G ratio. The corresponding I_D/I_G ratios of CNT and C-SF were 0.84 and 0.97, as shown in Fig. 2. The increase in the I_D/I_G ratio of C-SF was caused by the functionalization of CNT.

The functionalization of CNT and the formation of C-SF were further confirmed by FT-IR analyses. The FT-IR spectrum of pristine CNT showed a featureless signal, which indicated the absence of a functional group on the pristine CNT (Fig. 3a). After an acid-treatment, there were typical signals of oxygen containing functional groups which had formed on the surface of the CNT at 1172 cm^{-1} from the C—O stretching of the epoxy group, at 1712 cm^{-1} from C=O stretching of the carboxylic acid group, and at 3440 cm^{-1} from the O—H vibration of the hydroxyl group (Fig. 3a). The appearance of these functional groups verified the successful functionalization of CNT in good agreement with the surface charges of the CNT. The FT-IR spectrum of C-SF showed strong signals at 809 and 1112 cm^{-1} from the Si—O—Si stretching of silica and newly appeared peaks at 1569 and 1586 cm^{-1} from the O=C—N—H stretching of the amide group with the weakened C=O stretching of the carboxylic acid group (Fig. 3b). The difference in the FT-IR spectrum of the acid-treated CNT and the C-SF clearly revealed that the CNT was covalently bonded to the surface of the aminated SF.

A SEM analysis of the SF and acid-treated CNT showed the spherical shape of SF with a size ranging from 50 to 250 nm (Fig. 4a), along with the tubular shape of CNT which was significantly shorter from 10 μm to several hundreds of nm (Fig. 4b). The SEM images of C-SF exhibited closely-incorporated structures of the acid-treated CNT onto the surface of the aminated SF (Fig. 4c and d). SEM characterization also confirmed that both the functionalized CNT and the SF were tightly bonded together through covalent bonds. It is worth to note that the connected

structure of C-SF was stable even after repeated and prolonged sonication for dispersion. Fig. 5 shows the synthetic scheme of the carbonyl chloride-functionalized CNT, the aminated SF and their hybrid structures.

Meanwhile, Fig. 6 shows the sedimentation test results of the solutions including C-SF and pristine CNT. The test results showed that the dispersion of C-SF was significantly improved compared to that of the pristine CNT. The sedimentation of C-SF particles in the aqueous solution was mostly complete after 2 h, while that of the pristine CNT particles in the aqueous solution was observed to occur rapidly within 3 min.

5. Compressive strength of cementitious composites incorporating C-SF

Fig. 7 shows the compressive strength test results of the cementitious composites incorporating C-SF at 28 days. The compressive strength of the OPC specimen was similar to that of the specimen incorporating SF. It has been reported in previous studies that a proper amount of SF added to cementitious materials to improve the compressive strength was from 2 to 25% by the weight of cement [8,37]. The content of SF particles added to cementitious composites in the present study was less than 0.5 wt%. That is, the content of SF particles added to the SF specimen was too low to improve the compressive strength. Meanwhile, the compressive strength of the specimens incorporating C-SF was significantly improved compared to that of the OPC specimen. The fractional increases in the compressive strength of the C-SF 0.15, C-SF 0.25 and C-SF0.5 specimens compared to that of the OPC specimen were 104.7%, 128.9% and 107.6%, respectively. It has also been reported in previous studies that the fractional increases in the compressive strength of cementitious materials with a SF content less than 0.5 wt% compared to OPC specimens ranged from 5 to 20% [8,37,31]. That is, the improvement of the compressive strength induced by the addition of the C-SF was greater than that induced by the addition of SF particles.

6. Effect of C-SF on the characteristics of hydrates

Fig. 8 shows SEM images of the cementitious composites incorporating C-SF. It was observed in Fig. 8(a) that the C-SF particles were well distributed in the composite and that the SF synthesized with CNT was not dissolved. That is, the SF particles maintained their spherical shapes. It has been reported in previous studies that the SF added to the cementitious materials dissolved after 7 days [20]. Meanwhile, the SF synthesized with CNT was not observed in Fig. 8(b). Instead, it was observed that some parts of the CNT particles were embedded into the hydrates. It can be inferred from the results that the SF particles were dissolved and anchored between the CNT and the hydrates through a pozzolanic reaction.

Fig. 9 shows the nanoindentation test results of the cementitious composites incorporating C-SF. It should be noted that a
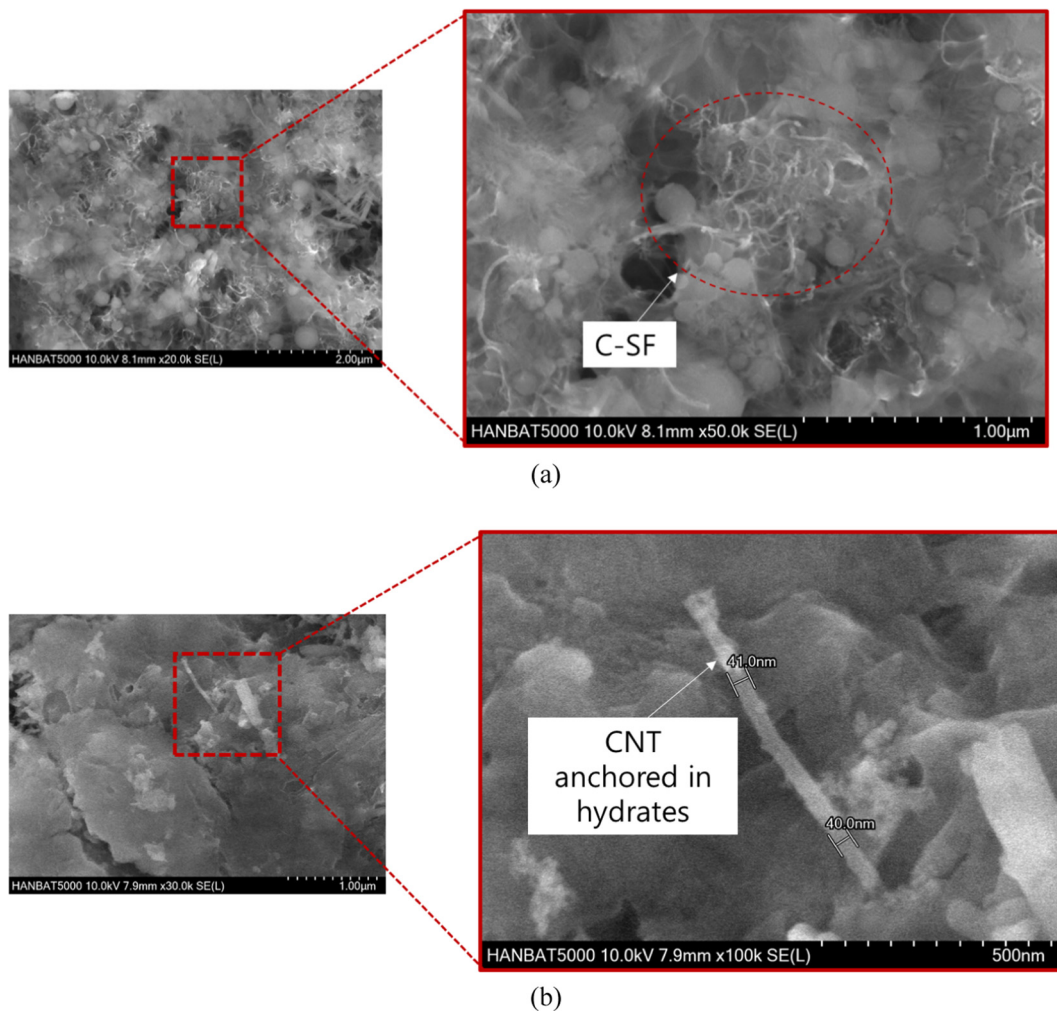

(a)

(b)

Fig. 8. SEM images of cementitious composites incorporating covalently synthesized CNT and silica fume at (a) 3 days of and (b) 28 days of curing.
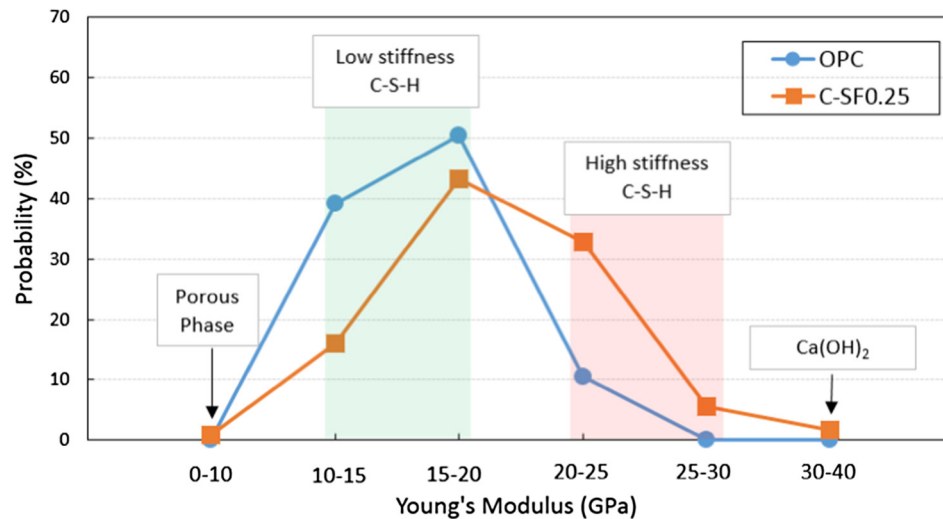
Fig. 9. Nanoindentation test results: probability plots of Young's modulus of cementitious composites incorporating covalently synthesized CNT and silica fume.

proper amount of SF and CNT added to cementitious materials to improve the compressive strength were from 2 to 25 wt% and lower than 0.2% by the weight of cement, respectively [8,37,11]. In addition, the improvement of compressive strength induced by the incorporation of SF and CNT was from 10 to 30% compared to cementitious materials without SF or CNT. However, the content of SF used here was lower than 0.5 wt% and the compressive strength of the composites incorporating SF was not improved compared to that of the composites without SF or CNT. Meanwhile, it was difficult to experimentally quantify the content of pristine CNT from C-SF in the present study and the improvement of compressive strength of cementitious composites incorporating pristine CNT in previous studies was clearly lower than that of cementitious composites incorporating C-SF. Therefore, the nanoindentation tests in the present study were conducted with OPC and C-SF0.25 samples. However, a further study is needed to quantify the content of pristine CNT from C-SF. The Young's modulus obtained from the nanoindentation test results represents the porous phase (0–10 GPa), low stiffness calcium silicate hydrate (C-S-H) phases (10–20 GPa), high stiffness C-S-H phases (20–30 GPa), portlandite (30–40 GPa) and unhydrated particles (100–170 GPa) [35,40,39,5,6,22]. The major binding hydrates in a cementitious composite are C-S-H phases which mainly affect the mechanical properties of cementitious materials [14]. The test results indicate that the addition of C-SF led to an increase in the high stiffness C-S-H in the cementitious composites, while low stiffness C-S-H mainly composed the hydrates in the OPC specimen. Overall, the SF synthesized with CNT acted as an anchor to improve the bond strength between the CNT and the hydrates, thereby improving the C-S-H stiffness. Consequently, the compressive strength of the composites with C-SF was clearly improved.

7. Concluding remarks

In the present study, aminated SF and carbonyl chloride functionalized CNT were covalently bonded by the formation of amide bridges. C-SF was added to cementitious composites and the mechanical characteristics of the composites incorporating the C-SF were thoroughly investigated. The relevant mechanism of the mechanical properties of the composites was discussed with nanoindentation and SEM analyses. The findings from the present study can be summarized as follows.

(1) The covalently bonded CNT and SF were well dispersed in the aqueous solution compared to pristine CNT particles.
(2) The compressive strength of cementitious composites incorporating C-SF was clearly improved compared to that of the OPC specimen, while the flexural strength of cementitious composites incorporating C-SF was similar to that of the OPC specimen.
(3) It was observed in SEM tests that C-SF was well distributed in the cementitious composites and that CNT on the surface of SF was anchored in the hydrates of the composites at 28 days of curing.
(4) Nanoindentation tests showed that the C-SF added to the cementitious composites improved the stiffness of the C-S-H phase in the composites.

It can be concluded that the addition of the C-SF contributed to a significant improvement of the nanomechanical properties of hydrates, thereby increasing the compressive strength of cementitious composites. Accordingly, the potential usage of cementitious composites incorporating C-SF may include weight-lightening of structural units due to the fact that the composites exhibit relatively high compressive strength with the enhanced dispersion of C-SF.

Conflict of interest

There are no conflicts to declare.

Acknowledgements

References

[1] K. Arroudj, A. Zenati, M.N. Oudjit, A. Bali, A. Tagnit-Hamou, Reactivity of fine quartz in presence of silica fume and slag, Engineering 3 (06) (2011) 569.

[2] S. Bal, S.S. Samal, Carbon nanotube reinforced polymer composites—a state of the art, Bull. Mater. Sci. 30 (4) (2007) 379–386.

[3] Y.W. Chan, S.H. Chu, Effect of silica fume on steel fiber bond characteristics in reactive powder concrete, Cem. Concr. Res. 34 (7) (2004) 1167–1172.

[4] F. Collins, J. Lambert, W.H. Duan, The influences of admixtures on the dispersion, workability, and strength of carbon nanotube–OPC paste mixtures, Cem. Concr. Compos. 34 (2) (2012) 201–207.

[5] G. Constantinides, The Elastic Properties of Calcium Leached Cement Pastes and Mortars: A Multi-Scale Investigation (Doctoral Dissertation, Massachusetts Institute of Technology), 2002.

[6] M.J. DeJong, F.J. Ulm, The nanogranular behavior of CSH at elevated temperatures (up to 700 C), Cem. Concr. Res. 37 (1) (2007) 1–12.

[7] P. Duan, Z. Shui, W. Chenm, C. Shen, Effects of metakaolin, silica fume and slag on pore structure, interfacial transition zone and compressive strength of concrete, Constr. Build. Mater. 44 (2013) 1–6.

[8] R. Duval, E.H. Kadri, Influence of silica fume on the workability and the compressive strength of high-performance concretes, Cem. Concr. Res. 28 (4) (1998) 533–547.

[9] R. Hamzaoui, S. Guessasma, B. Mecheri, A.M. Eshtiaghi, A. Bennabi, Microstructure and mechanical performance of modified mortar using hemp fibres and carbon nanotubes, Mater. Des. 56 (2014) 60–68.

[10] B.T. Kelly, Physics of Graphite, Applied Science, London, 1981.

[11] H.K. Kim, I.W. Nam, H.K. Lee, Enhanced effect of carbon nanotube on mechanical and electrical properties of cement composites by incorporation of silica fume, Compos. Struct. 107 (2014) 60–69.

[12] G.M. Kim, I.W. Nam, H.N. Yoon, H.K. Lee, Effect of superplasticizer type and siliceous materials on the dispersion of carbon nanotube in cementitious composites, Compos. Struct. 185 (2018) 264–272.

[13] G.M. Kim, B.J. Yang, K.J. Cho, E.M. Kim, H.K. Lee, Influences of CNT dispersion and pore characteristics on the electrical performance of cementitious composites, Compos. Struct. 164 (2017) 32–42.

[14] G.M. Kim, B.J. Yang, G.U. Ryu, H.K. Lee, The electrically conductive carbon nanotube (CNT)/cement composites for accelerated curing and thermal cracking reduction, Compos. Struct. 158 (2016) 20–29.

[15] Y.K. Kim, D.H. Min, Fabrication of alternating multilayer films of graphene oxide and carbon nanotube and its application in mechanistic study of laser desorption/ionization of small molecules, ACS Appl. Mater. Interfaces 4 (4) (2012) 2088–2095.

[16] M.S. Konsta-Gdoutos, Z.S. Metaxa, S.P. Shah, Highly dispersed carbon nanotube reinforced cement based materials, Cem. Concr. Res. 40 (7) (2010) 1052–1059.

[17] M.S. Konsta-Gdoutos, Z.S. Metaxa, S.P. Shah, Multi-scale mechanical and fracture characteristics and early-age strain capacity of high performance carbon nanotube/cement nanocomposites, Cem. Concr. Compos. 32 (2) (2010) 110–115.

[18] S. Kumar, P. Kolay, S. Malla, S. Mishra, Effect of multiwalled carbon nanotubes on mechanical strength of cement paste, J. Mater. Civ. Eng. 24 (1) (2011) 84–91.

[19] G. Liu, Y. Zhao, K. Deng, Z. Liu, W. Chu, J. Chen, Y. Yang, K. Zheng, H. Huang, W. Ma, L. Song, H. Yang, C. Gu, G. Rao, C. Wang, S. Xie, L. Sun, Highly dense and perfectly aligned single-walled carbon nanotubes fabricated by diamond wire drawing dies, Nano Lett. 8 (2008) 1071–1075.

[20] P.K. Mehta, O.E. Gjørv, Properties of Portland cement concrete containing fly ash and condensed silica-fume, Cem. Concr. Res. 12 (5) (1982) 587–595.

[21] H.E. Misak, R. Asmatulu, M. O'Malley, E. Jurak, S. Mall, Functionalization of carbon nanotube yarn by acid treatment, Int. J. Smart Nano Mater. 5 (1) (2014) 34–43.

[22] P. Mondal, S.P. Shah, L. Marks, A reliable technique to determine the local mechanical properties at the nanoscale for cementitious materials, Cem. Concr. Res. 37 (10) (2007) 1440–1444.

[23] M.S. Morsy, S.H. Alsayed, M. Aqel, Hybrid effect of carbon nanotube and nano-clay on physico-mechanical properties of cement mortar, Constr. Build. Mater. 25 (1) (2011) 145–149.

[24] S. Musso, J.M. Tulliani, G. Ferro, A. Tagliaferro, Influence of carbon nanotubes structure on the mechanical behavior of cement composites, Compos. Sci. Technol. 69 (11) (2009) 1985–1990.

[25] P.R. Mudimela, L.I. Nasibulina, A.G. Nasibulin, A. Cwirzen, M. Valkeapää, K. Habermehl-Cwirzen, O.V. Tolochko, Synthesis of carbon nanotubes and nanofibers on silica and cement matrix materials, J. Nanomater. 2009 (2009) 29.

[26] A.G. Nasibulin, S.D. Shandakov, L.I. Nasibulina, A. Cwirzen, P.R. Mudimela, K. Habermehl-Cwirzen, Y. Tian, A novel cement-based hybrid material, New J. Phys. 11 (2) (2009) 023013.

[27] T. Nochaiya, A. Chaipanich, Behavior of multi-walled carbon nanotubes on the porosity and microstructure of cement-based materials, Appl. Surf. Sci. 257 (6) (2011) 1941–1945.

[28] S. Parveen, P. Kolay, S. Malla, M.C. Paiva, Microstructure and mechanical properties of carbon nanotube reinforced cementitious composites developed using a novel dispersion technique, Cem. Concr. Res. 73 (2015) 215–227.

[29] N. Phonthammachai, J.C. Kah, G. Jun, C.J. Sheppard, M.C. Olivo, S.G. Mhaisalkar, T.J. White, Synthesis of contiguous silica-gold core-shell structures: critical parameters and processes, Langmuir 24 (9) (2008) 5109–5112.

[30] C.S. Poon, S.C. Kou, L. Lam, Compressive strength, chloride diffusivity and pore structure of high performance metakaolin and silica fume concrete, Constr. Build. Mater. 20 (10) (2006) 858–865.

[31] Y. Qing, Z. Zenan, K. Deyu, C. Rongshen, Influence of nano-SiO 2 addition on properties of hardened cement paste as compared with silica fume, Constr. Build. Mater. 21 (3) (2007) 539–545.

[32] A.A. Ramezanianpour, V.M. Malhotra, Effect of curing on the compressive strength, resistance to chloride-ion penetration and porosity of concretes incorporating slag, fly ash or silica fume, Cem. Concr. Compos. 17 (2) (1995) 125–133.

[33] B.B. Sabir, S. Wild, J. Bai, Metakaolin and calcined clays as pozzolans for concrete: a review, Cem. Concr. Compos. 23 (6) (2001) 441–454.

[34] J.P. Salvetat, J.M. Bonard, N.H. Thomson, A.J. Kulik, L. Forro, W. Benoit, L. Zuppiroli, Mechanical properties of carbon nanotubes, Appl. Phys. A 69 (3) (1999) 255–260.

[35] S.P. Shah, M.S. Konsta-Gdoutos, Z.S. Metaxa, P. Mondal, Nanoscale modification of cementitious materials, Nanotechnol. Constr. 3 (2009) 125–130.

[36] H.A. Toutanji, N. Delatte, S. Aggoun, R. Duval, A. Danson, Effect of supplementary cementitious materials on the compressive strength and durability of short-term cured concrete, Cem. Concr. Res. 34 (2) (2004) 311–319.

[37] H.A. Toutanji, T. El-Korchi, The influence of silica fume on the compressive strength of cement paste and mortar, Cem. Concr. Res. 25 (7) (1995) 1591–1602.

[38] M.J. Treacy, T.W. Ebbesen, J.M. Gibson, Exceptionally high Young's modulus observed for individual carbon nanotubes, Nature 381 (1996) 678–680.

[39] F.J. Ulm, Z.P. Bazant, F.H. Wittman, Creep, Shrinkage, and Durability Mechanics of Concrete and Other Quasi-Brittle Materials, Elsevier, 2001.

[40] K. Velez, S. Maximilien, D. Damidot, G. Fantozzi, F. Sorrentino, Determination by nanoindentation of elastic modulus and hardness of pure constituents of Portland cement clinker, Cem. Concr. Res. 31 (4) (2001) 555–561.

[41] Q. Zhang, G. Chen, S.F. Yoon, J. Ahn, S.G. Wang, Q. Zhou, J.Q. Li, Thermal conductivity of multiwalled carbon nanotubes, Phys. Rev. B 66 (16) (2002) 165440.